

Novel orbital selective phase transition induced by different magnetic states: A dynamical cluster approximation study

Hunpyo Lee,¹ Yu-Zhong Zhang,^{1,2} Harald O. Jeschke,¹ and Roser Valentí¹

¹*Institut für Theoretische Physik, Goethe-Universität Frankfurt,
Max-von-Laue-Straße 1, 60438 Frankfurt am Main, Germany*

²*Department of Physics, Tongji University, Shanghai, 200092 P. R. China*
(Dated: November 2, 2010)

By considering the dynamical cluster approximation combined with the continuous time quantum Monte Carlo algorithm, we analyze the behavior of a degenerate two-orbital anisotropic Hubbard model at half filling where both orbitals have equal bandwidths and one orbital is constrained to be paramagnetic (PM) (PM orbital), while the second one is allowed to have an antiferromagnetic (AF) solution (AF orbital). As the interaction increases, novel orbital selective phase transitions induced by different magnetic states in different orbitals appear regardless of the strength of the Ising Hund's rule coupling J_z . Moreover, the PM orbital undergoes a transition from a Fermi liquid (FL) to a Mott insulator through an intermediate non-FL phase while the AF orbital shows a transition from a FL to an AF insulator through an intermediate AF metallic phase. Finally, the phase diagram of the model is presented and possible applications of the model to some aspects of the physics of iron pnictides are discussed.

PACS numbers: 71.10.Fd, 71.27.+a, 71.30.+h, 71.10.Hf

The existence of an orbital selective phase transition (OSPT) induced by the interplay of a narrow band of localized electrons and a wide band of itinerant electrons has evoked considerable interest since the discovery of exotic phase transitions in $\text{Ca}_{2-x}\text{Sr}_x\text{RuO}_4$ [1, 2]. Presently, OSPT are being intensively investigated as an alternative to conventional Mott transitions happening simultaneously in all orbitals in correlated systems [3–11]. Previous works on OSPT were either based on degenerate orbitals with inequivalent bandwidths at integer filling [3–9] or focused on orbitals with degeneracies lifted completely or partially by the crystal field splitting at different fillings [10, 11]. In the present work, a new mechanism for an OSPT induced by different magnetic states in different orbitals is proposed.

In order to verify the proposed new scenario for the OSPT, we consider a degenerate two-orbital anisotropic Hubbard model at half filling where both orbitals have equal bandwidths and one orbital is constrained to be paramagnetic (PM) (PM orbital), while the second one is allowed to have an antiferromagnetic (AF) solution (AF orbital). We employ the dynamical cluster approximation (DCA) [12] with a cluster size of $N_c = 4$ in combination with a weak-coupling continuous time quantum Monte Carlo algorithm [13] which expands the interaction term. Such an approach ensures the consideration of the dynamical fluctuations and the inclusion of a symmetry-breaking state as well as spatial fluctuations which cannot be captured in most of previous OSPT works using a single-site dynamical mean field theory (DMFT) [3–6, 10, 11].

We find a novel OSPT: In the PM orbital, a phase transition from a Fermi liquid (FL) to a non-FL state followed by a Mott metal-to-insulator transition (MIT)

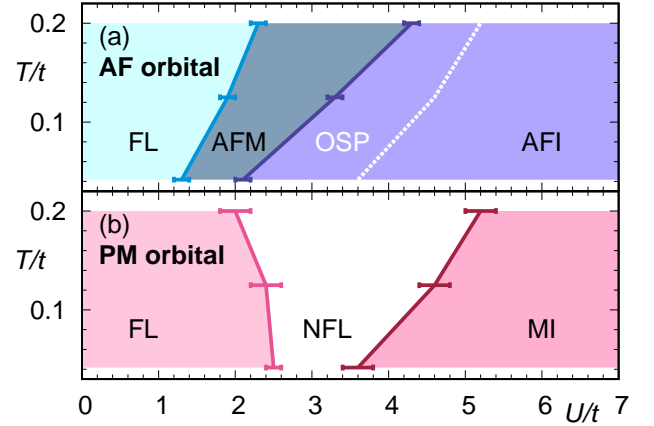


FIG. 1. The $U - T$ phase diagram of (a) AF and (b) PM orbitals for $J_z = U/8$ and $U' = 3U/4$. The non-FL and AF metal are determined by the self-energy neither showing divergent behavior nor approaching zero as the Matsubara frequency goes to zero and the spin-dependent symmetry breaking field remaining finite in the metallic state, respectively.

is detected, while in the AF orbital two phase transitions from a PM metal to an AF insulator through an AF metallic state are observed, regardless of the strength of the Ising-type Hund's rule coupling J_z . All the transitions occur at different critical values of U/t . Note that here the OSPT occurs when the PM orbital undergoes a Mott MIT while the AF orbital remains an AF insulator. Furthermore, we also discuss the nature of the Mott MIT in the PM orbital at $J_z = 0$ where the ferromagnetic interaction between PM and AF orbitals vanishes. Such a consideration simultaneously allows for the study of (i) strong orbital fluctuations between PM and AF orbitals as well as (ii) the effect that the AF order in

the AF orbital induces on the PM orbital. Moreover, comparable to the single-orbital Hubbard model within a small cluster [14–16], the cooperation between the spatial AF order due to perfect nesting and frustration induced by short-range spatial fluctuations remains in our model. Therefore, it is interesting to compare the results of the single-orbital Hubbard model with those of the two-orbital Hubbard model. While the single-orbital Hubbard model shows a first-order Mott MIT [14, 15], we observe a continuous Mott MIT in the PM orbital with a critical interaction $U_c/t = 4.0$ close to that obtained for the single-orbital system by the same DCA method with a cluster size of $N_c = 4$ [15, 17]. Finally, we discuss the relevance of the small magnetic moment in the AF orbital in the context of the experimentally observed ordered magnetic moment in iron pnictides which has a reduced value in comparison to density functional theory (DFT) calculations [18–20].

The degenerate two-orbital anisotropic Hubbard model with a PM and an AF orbital at half-filling on the square lattice can be written as

$$H = - \sum_{\langle ij \rangle m \sigma} t_m c_{im\sigma}^\dagger c_{jm\sigma} + U \sum_{im} n_{im\uparrow} n_{im\downarrow} + \sum_{i\sigma\sigma'} (U' - \delta_{\sigma\sigma'} J_z) n_{i1\sigma} n_{i2\sigma'}, \quad (1)$$

where $c_{im\sigma}$ ($c_{im\sigma}^\dagger$) is the annihilation (creation) operator of an electron with spin σ at the i -th site with orbital index $m = (1, 2)$. t_m is the hopping matrix element between site i and j , U and U' are intra-orbital and inter-orbital Coulomb repulsion integrals, respectively, and $J_z n_{i1\sigma} n_{i2\sigma}$ is the Ising-type Hund's rule coupling term. The spin-flip and pair-hopping processes are neglected and the bandwidth is $W = 8$ ($t = 1$) in our calculation. In order to simulate our anisotropic Hubbard model with a PM and an AF orbital, a spin-dependent symmetry breaking field is applied on the AF orbital in the first iteration, while we always keep the PM solution under the condition of $\overline{G}_{PM}(\mathbf{K}, i\omega_n) = \frac{1}{2}(\overline{G}_\uparrow(\mathbf{K}, i\omega_n) + \overline{G}_\downarrow(\mathbf{K}, i\omega_n))$ for the PM orbital at each iteration. Here $\overline{G}(\mathbf{K}, i\omega_n)$ is the cluster Green's function and it is obtained from the DCA and Dyson equations in around fifteen DCA iterations.

First, we would like to discuss the phase diagram for $J_z = U/8$ and $U' = 3U/4$ in the $U - T$ plane shown in Fig. 1. Analogous to the phase diagram of the single-orbital Hubbard model with a PM solution obtained from cluster-DMFT with $N_c = 4$ [14], we observe that the FL, non-FL and Mott insulator phases are present in the PM orbital. The metallic regions are shrunk due to the enhancement of spatial AF correlations with decreasing temperature. The main difference between single-orbital and our two-orbital Hubbard model is that the first-order MIT, which is present in the single-orbital Hubbard model, is replaced by a continuous MIT in the two-orbital

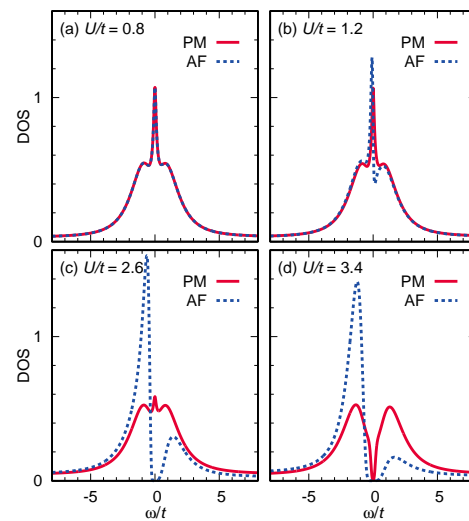


FIG. 2. Density of states (DOS) for different values of the interaction strength U/t , with $U' = U/2$ and $J_z = U/4$ at $T/t = 1/24$. Here, only the DOS for spin up is present when the AF orbital is in an AF state.

Hubbard model (see Fig. 1 (b)). The coupling between the PM orbital with spatial AF correlations and the AF orbital with AF order suppresses the first-order transition. Furthermore, in the weak-coupling region, while the AF insulator is present in the cluster-DMFT calculation of the single-orbital Hubbard model when an AF solution is permitted [21], in our AF orbital the AF symmetry breaking field is completely suppressed due to the thermal and orbital fluctuations between PM and AF orbitals (see Fig. 1 (a)). In fact, in the intermediate region the AF orbital shows an AF metallic phase and as the interaction U/t is increased, the AF insulator state is reached. The orbital selective phase where a metallic state in the PM orbital and an insulating state in the AF orbital coexist, is clearly observed in the intermediate regime. Such a phase is induced by different magnetic states in the two orbitals. This mechanism is distinct from previously proposed ones, such as change of filling in non-degenerate or partially degenerate orbitals [10, 11], variation of bandwidth in different orbitals [3–8] or differences of frustration strength in different orbitals [9].

In the following, we will analyze the various states in our phase diagram. Figs. 2 (a)-(d) show the density of states (DOS) for the two orbitals for several values of the interaction strengths U/t with $U' = U/2$ and $J_z = U/4$ at $T/t = 1/24$. Here the maximum entropy method for analytical continuation was applied. In the weak-coupling region ($U/t = 0.8$) both the PM and the AF orbital are in the PM metallic phase. The AF state in the AF orbital completely disappears due to orbital fluctuations and temperature effects. This results in the same DOS for both orbitals including a quasiparticle peak at the Fermi level as shown in Fig. 2 (a). As the interaction increases ($U/t = 1.2$), the AF orbital - while remain-

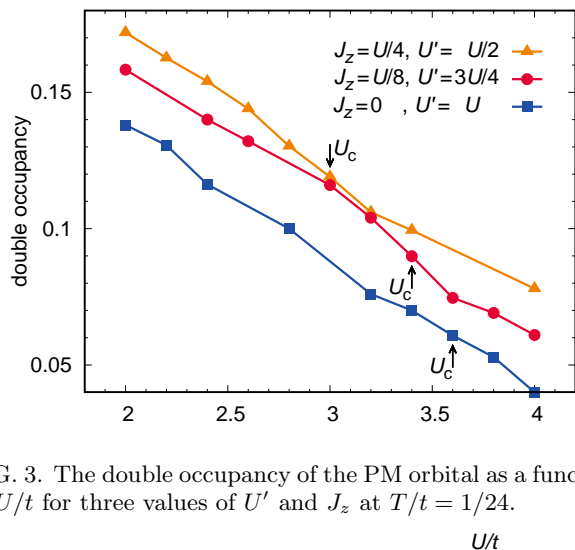


FIG. 3. The double occupancy of the PM orbital as a function of U/t for three values of U' and J_z at $T/t = 1/24$.

ing metallic - starts to display AF order as shown in Fig. 2 (b). In this case, the spin up DOS is pairwise equal to the spin down DOS on each site due to the appearance of antiferromagnetism. The PM orbital remains in the PM metallic phase with a quasiparticle peak at the Fermi level. In the intermediate region at $U/t = 2.6$ (Fig. 2 (c)), the orbital selective phase is present where the metallic PM orbital coexists with the insulating AF orbital. When the interaction is further increased to the strong-coupling region ($U/t = 3.4$), insulating states appear in both orbitals as displayed in Fig. 2 (d). Note that we found the OSPT behavior for all investigated values of J_z .

Next, we would like to clarify the nature of the Mott MIT in the PM orbital. In the case of the single-orbital Hubbard model, the double occupancy shows hysteresis with coexistence regions indicating a first-order phase transition [14]. Since our two-orbital system allows for additional orbital degrees of freedom, it is interesting to check whether the nature of the transition is changed due to the coupling between AF and PM orbitals. In Fig. 3, we plot the double occupancy as a function of U/t with different U' and J_z at $T/t = 1/24$. While U_c/t increases from 3.0 to 3.4 and 3.6 when J_z is decreased from $U/4$ to $U/8$ and to 0 with the constraint of $U = U' + 2J_z$, in none of the cases a signature of hysteresis in the double occupancy is found. The disappearance of the first-order transition is attributed to (i) the interaction between the orbitals and (ii) the cooperation of spatial AF correlations in the PM orbital and AF order in the AF orbital at all values of J_z .

Recently, the non-FL behavior in the multi-orbital as well as in the single-orbital Hubbard model has been extensively studied within DMFT or its cluster extension [5, 8, 11, 14–16, 22–24]. Using the maximum entropy method suggested by Wang *et al.* [25] for the analytical continuation of the self-energy, we analyze the self-energy $\Sigma(\omega)$ at the Fermi surface $\mathbf{K}(\pi, 0)$ of the PM orbital as

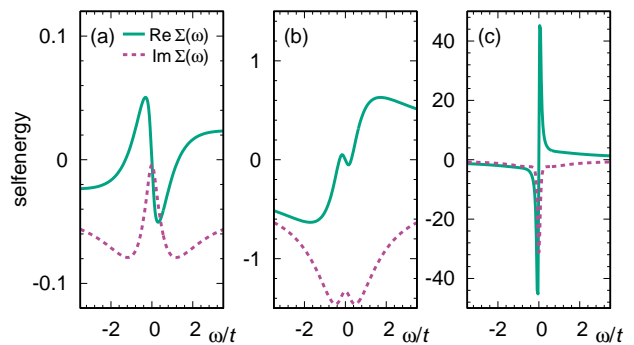


FIG. 4. (a)-(c) Self-energies at the Fermi surface $\mathbf{K}(\pi, 0)$ as a function of real frequency ω/t at (a) $U/t = 0.8$, (b) $U/t = 2.6$ and (c) $U/t = 3.4$ for $U' = U/2$, $J_z = U/4$ at $T/t = 1/24$ on the PM orbital.

a function of the real frequency ω (see Figs. 4 (a)-(c)) for $U' = U/2$, $J_z = U/4$ at $T/t = 1/24$. In Fig. 4 (a), $\text{Im}\Sigma(\omega = 0)$ approaches zero indicating a FL behavior. Upon increasing the interaction in Fig. 4 (b), the system still shows metallic behavior but $\text{Im}\Sigma(\omega = 0)$ has a finite value. This indicates a non-FL behavior. In the strong-coupling region ($U/t = 3.4$), the self-energy $\text{Im}\Sigma(\omega = 0)$ diverges (Fig. 4 (c)) and the system is in a Mott insulating state. Also shown in Figs. 4 (a)-(c) is the $\text{Re}\Sigma(\omega)$ obtained from the Kramers-Kronig relation. From these results we infer that the gap opening in the PM orbital is caused by a blocking of the electron delocalization due to the Coulomb repulsion (Mott insulator), while in the AF orbital the quasi-particle peak is split into two parts above and below the Fermi level due to the antiferromagnetism with a gap of $\Delta \approx mU$ (AF insulator), where m is the magnetization and U is the interaction strength. Here we would like to stress that the gap opening in the AF orbital – which favors antiferromagnetism – happens at a lower interaction strength than it happens in the PM orbital. Therefore, a Mott MIT occurs in the PM orbital while the AF orbital remains an AF insulator. As mentioned above, this indicates a novel OSPT driven by different magnetic states in different orbitals.

Finally, we analyze the AF metallic phase in the AF orbital at intermediate couplings. Unlike the high- T_c cuprates with an AF insulating state in the normal phase, the undoped iron-based superconductors show AF metallic behavior with a small ordered magnetic moment. DFT calculations [18–20] overestimate the values of the ordered magnetic moment compared to those obtained from experiments. With the consideration of an artificially negative U in the DFT calculations, the small magnetic moment is recovered [26, 27]. Nevertheless the mechanism for the reduced ordered magnetic moment still remains controversial [28–33]. Very recently, the authors proposed a mechanism of coupling between frustrated and unfrustrated orbitals within a two-orbital Hubbard model, solved by single-site DMFT [9] as a pos-

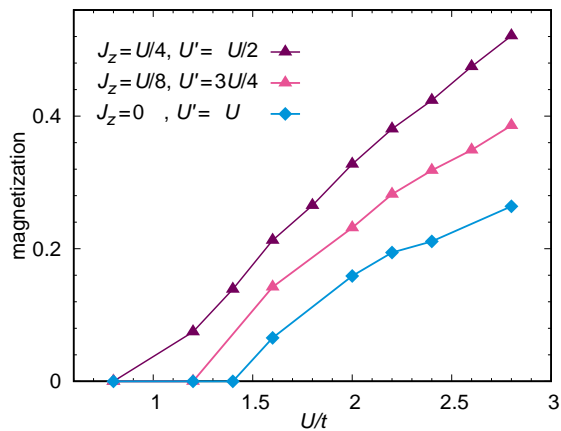


FIG. 5. The staggered magnetization of the AF orbital as a function of U/t for three values of U' and J_z .

sible mechanism for the reduced magnetic moment and the AF metallic state. In the present work we study a related model (Eq. (1)) by DCA where spatial fluctuations – absent in the single-site DMFT calculation – are partially considered. Instead of introducing an additional next-nearest-neighbor hopping for frustration, here we keep one orbital always in the PM state. This can be viewed as an effective frustration due to the suppression of long-range correlations by the small cluster size [14]. In Fig. 5 we present the staggered magnetization in the AF orbital as a function of U/t with different U' and J_z for $T/t = 1/24$. The critical U_c/t for the onset of the AF state at $J_z = 0$ is larger than that at finite J_z values because of the strong orbital fluctuations at $J_z = 0$. We observe that, as the interaction strength is increased, the staggered magnetization increases continuously for all values of J_z and remains small in the range $U/t = 1.5-2.5$. This is consistent with DMFT results [9].

In conclusion, we have studied the two-orbital Hubbard model at half filling where one orbital is constrained to be in the PM state and the second orbital is allowed to have an AF solution. Analysis of double occupancy, magnetization and DOS shows that as U/t increases, while a continuous Mott MIT through non-FL behavior is observed in the PM orbital, two phase transitions (PM metal to AF metal and AF metal to AF insulator) are detected in the AF orbital. We find a novel orbital selective phase transition where a MIT occurs in the PM orbital while the AF orbital remains an AF insulator. We ascribe the OSPT detected in this work to the different magnetic states in the different orbitals since other effects such as different bandwidths, crystal field splitting and change of band filling have been avoided. Even with inclusion of spatial fluctuations, the AF metal still survives in the AF orbital in a certain range of interaction strengths. These results support the scenario of a reduced ordered magnetic moment and the existence of an AF metallic state in the Fe pnictides driven by coupling between frustrated and

unfrustrated orbitals [9]. Finally, by investigating the self-energy as a function of real frequency ω/t , we identify an interaction regime where non-FL behavior can be observed in the PM orbital.

Acknowledgments.- We would like to thank the Deutsche Forschungsgemeinschaft for financial support through grants SFB/TRR 49, FOR 1346 and SPP 1458 and the Helmholtz Association for support through HA216/EMMI.

-
- [1] S. Nakatsuji and Y. Maeno, Phys. Rev. Lett. **84**, 2666 (2000).
 - [2] V. I. Anisimov, I. A. Nekrasov, D. E. Kondakov, T. M. Rice, and M. Sigrist, Eur. Phys. J. B **25**, 191 (2002).
 - [3] A. Koga, N. Kawakami, T. M. Rice, and M. Sigrist, Phys. Rev. Lett. **92**, 216402 (2004).
 - [4] C. Knecht, N. Blümer, and P. G. J. van Dongen, Phys. Rev. B **72**, 081103 (2005).
 - [5] S. Biermann, L. de' Medici, and A. Georges, Phys. Rev. Lett. **95**, 206401 (2005).
 - [6] A. Liebsch, Phys. Rev. Lett. **95**, 116402 (2005).
 - [7] K. Bouadim, G. G. Batrouni, and R. T. Scalettar, Phys. Rev. Lett. **102**, 226402 (2009).
 - [8] H. Lee, Y.-Z. Zhang, H. O. Jeschke, R. Valentí, and H. Monien, Phys. Rev. Lett. **104**, 026402 (2010).
 - [9] H. Lee, Y.-Z. Zhang, H. O. Jeschke, and R. Valentí, Phys. Rev. B **81**, 220506(R) (2010).
 - [10] P. Werner and A. J. Millis, Phys. Rev. Lett. **99**, 126405 (2007).
 - [11] L. de' Medici, S. R. Hassan, M. Capone, and X. Dai, Phys. Rev. Lett. **102**, 126401 (2009).
 - [12] T. Maier, M. Jarrell, T. Pruschke, and M. H. Hettler, Rev. Mod. Phys. **77**, 1027 (2005).
 - [13] A. N. Rubtsov, V. V. Savkin, and A. I. Lichtenstein, Phys. Rev. B **72**, 035122 (2005).
 - [14] H. Park, K. Haule, and G. Kotliar, Phys. Rev. Lett. **101**, 186403 (2008).
 - [15] E. Gull, P. Werner, X. Wang, M. Troyer, and A. J. Millis, Europhys. Lett. **84**, 37009 (2008).
 - [16] Y.-Z. Zhang and M. Imada, Phys. Rev. B **76**, 045108 (2007).
 - [17] C. Lin and A. J. Millis, Phys. Rev. B **79**, 205109 (2009).
 - [18] I. I. Mazin, M. D. Johannes, L. Boeri, K. Koepernik, and D. J. Singh, Phys. Rev. B **78**, 085104 (2008).
 - [19] I. Opahle, H. C. Kandpal, Y. Zhang, C. Gros, and R. Valentí, Phys. Rev. B **79**, 024509 (2009).
 - [20] Y.-Z. Zhang, H. C. Kandpal, I. Opahle, H. O. Jeschke, and R. Valentí, Phys. Rev. B **80**, 094530 (2009).
 - [21] A. Fuhrmann, S. Okamoto, H. Monien, and A. J. Millis, Phys. Rev. B **75**, 205118 (2007).
 - [22] H. Ishida and A. Liebsch, Phys. Rev. B **81**, 054513 (2010).
 - [23] P. Werner, E. Gull, M. Troyer, and A. J. Millis, Phys. Rev. Lett. **101**, 166405 (2008).
 - [24] T. A. Costi and A. Liebsch, Phys. Rev. Lett. **99**, 236404 (2007).
 - [25] X. Wang, E. Gull, L. de' Medici, M. Capone, and A. Millis, Phys. Rev. B **80**, 045101 (2009).
 - [26] J. Ferber, Y.-Z. Zhang, H. O. Jeschke, and R. Valentí,

- Phys. Rev. B **82**, 165102 (2010).
- [27] G. Li, B. S. Conner, S. Weyeneth, N. D. Zhigadlo, S. Katorych, Z. Bukowski, J. Karpinski, D. J. Singh, M. D. Johannes, and L. Balicas, arxiv/1009.1408 (unpublished).
- [28] Q. Si and E. Abrahams, Phys. Rev. Lett. **101**, 076401 (2008).
- [29] Y.-Z. Zhang, I. Opahle, H. O. Jeschke, and R. Valentí, Phys. Rev. B **81**, 094505 (2010).
- [30] E. Bascones, M. Calderón, and B. Valenzuela, Phys. Rev. Lett. **104**, 227201 (2010).
- [31] F. Yang, S.-P. Kou, and Z.-Y. Weng, Phys. Rev. B **81**, 245130 (2010).
- [32] T. Misawa, K. Nakamura, and M. Imada, arxiv/1006.4812 (unpublished).
- [33] Z. P. Yin, K. Haule, and G. Kotliar, arxiv/1007.2867 (unpublished).